Early suppression of adipocyte lipid turnover induces immunometabolic modulation in cancer cachexia syndrome

Felipe Santos Henriques,[*,†,1] Rogério Antônio Laurato Sertié,[‡,1] Felipe Oliveira Franco,[*] Pamela Knobl,[*] Rodrigo Xavier Neves,[§] Sandra Andreotti,[‡] Fabio Bessa Lima,[‡] Adilson Guilherme,[‡] Marilia Seelaender,[§] and Miguel Luiz Batista, Jr.[*,2]

[*]Laboratory of Adipose Tissue Biology, Integrated Group of Biotechnology, University of Mogi das Cruzes, São Paulo, Brazil; [†]Program in Molecular Medicine, University of Massachusetts Medical School, Worcester, Massachusetts, USA; and [‡]Laboratory of Physiology and [§]Cancer Metabolism Research Group, Institute of Biomedical Sciences, University of São Paulo, São Paulo, Brazil

ABSTRACT: Cancer cachexia is a multifactorial syndrome characterized by body weight loss, atrophy of adipose tissue (AT) and systemic inflammation. However, there is limited information regarding the mechanisms of immunometabolic response in AT from cancer cachexia. Male Wistar rats were inoculated with 2×10^7 of Walker 256 tumor cells [tumor bearing (TB) rats]. The mesenteric AT (MeAT) was collected on d 0, 4, 7 (early stage), and 14 (cachexia stage) after tumor cell injection. Surgical biopsies for MeAT were obtained from patients who had gastrointestinal cancer with cachexia. Lipolysis showed an early decrease in glycerol release in TB d 4 (TB4) rats in relation to the control, followed by a 6-fold increase in TB14 rats, whereas *de novo* lipogenesis was markedly lower in the incorporation of glucose into fatty acids in TB14 rats during the development of cachexia. CD11b and CD68 were positive in TB7 and TB14 rats, respectively. In addition, we found cachexia stage results similar to those of animals in MeAT from patients: an increased presence of $CD68^+$, $iNOS2^+$, $TNF\alpha^+$, and HSL^+ cells. In summary, translational analysis of MeAT from patients and an animal model of cancer cachexia enabled us to identify early disruption in Adl turnover and subsequent inflammatory response during the development of cancer cachexia.—Henriques, F. S., Sertié, R. A. L., Franco, F. O., Knobl, P., Neves, R. X., Andreotti, S., Lima, F. B., Guilherme, A., Seelaender, M., Batista, M. L., Jr. Early suppression of adipocyte lipid turnover induces immunometabolic modulation in cancer cachexia syndrome. FASEB J. 31, 1976–1986 (2017). www.fasebj.org

KEY WORDS: ***de novo* lipogenesis · lipolysis · inflammation · adipose tissue**

Cancer cachexia (CC) is a multifactorial syndrome characterized by unintentional loss of adipose tissue (AT) and skeletal muscle, which cannot be fully reversed by conventional nutritional support and leads to progressive functional impairment (1, 2). This paraneoplastic syndrome affects ~50% of patients with cancer, may account for 20–25% of all cancer-attributed deaths, and is the primary cause of asthenia, respiratory complications, poor response to chemotherapy, increased susceptibility to infection, and poor quality of life in these patients (3).

At present, the loss of body weight in CC has been thought to be a result of profound changes in metabolic pathways of tissues and organs, which cannot be solely explained by enhanced energy expenditure or malnutrition (4). In this regard, the role of early AT dysfunction seems to have gained importance in the onset and progress of many alterations induced by the syndrome (5, 6). Different mechanistic possibilities have been proposed to explain the changes in AT in cachexia: for example, increase in lipolytic activity, decrease in the activity of lipoprotein lipase (LPL), reduction of *de novo* lipogenesis, and, consequently, decreased lipid [triacylglycerol (TG)] deposition (4, 7). In addition, alterations in AT metabolism have been recently described as suggesting a browning

ABBREVIATIONS: ACC, acetyl-CoA carboxylase; Adl, adipocyte lipid; AT, adipose tissue; ATGL, adipose triglyceride lipase; BMI, body mass index; BSA, bovine serum albumin; CCL, C-C motif chemokine ligand; CD, cluster of differentiation; CIDE, cell death-inducing DFFA-like effector; CXCL, C-X-C motif chemokine ligand; FA, fatty acid; FASN, fatty acid synthase; HSL, hormone-sensitive lipase; iNOS, inhibitory NOS; ITT, insulin tolerance test; LPL, lipoprotein lipase; MeAT, mesenteric adipose tissue; SVF, stromal-vascular fraction; TB, tumor-bearing; TB4/7/14, tumor-bearing day 4/7/14; TG, triacylglycerol; WSC, weight-stable cancer

[1] These authors contributed equally to this work.

[2] Correspondence: Avenida Doutor Cândido Xavier de Almeida Souza, 200, Centro Cívico, Mogi das Cruzes, São Paulo 08780-911, Brazil. E-mail: migueljr4@me.com

doi: 10.1096/fj.201601151R

This article includes supplemental data. Please visit *http://www.fasebj.org* to obtain this information.

0892-6638/17/0031-1976 © FASEB

process of white AT in cachexia (8, 9), with reduced adipogenesis, AT turnover (5, 10, 11), and enhanced inflammatory signaling (12, 13).

Adipocyte lipid (Adl) turnover determines AT mass [*i.e.*, the balance between incorporation and removal of TG into adipocytes, in which lipolysis (hydrolysis of intracellular TGs)] is the most important factor for lipid removal (14). In CC, human and animal models (15) have shown an increased rate of lipid mobilization, and longitudinal studies have shown that patients with CC lose AT mass before wasting of the muscle mass can be detected (16). In addition to that, an accelerated rate of AT loss is believed to be associated with shorter survival time during cancer progression (17). However, few studies have addressed the possible putative mechanisms behind the impairment of Adl turnover, and very little is known about how these factors contribute to the body weight loss observed during cancer cachexia development.

It has been proposed that chronic systemic inflammation in response to the progression of CC has a relevant contribution from AT, as we and others have shown (10, 12, 18, 19). A very early down-regulation of adipogenic and lipogenic (5, 20) pathways, as well as of browning genes (8), has been shown in the AT in a murine cachexia model. In the cachectic stage, AT remodeling is characterized by the presence of adipocyte atrophy, followed by fibrosis and increased inflammatory cell infiltrate, as shown in both murine models (5, 20) and patients with CC (10). In the latter, immune cell infiltration in the tissue was characterized by the presence of crown-like structures composed of $CD68^+$ macrophages surrounding adipocytes and by an increased number of $CD3^+$ lymphocytes, more evident in the fibrotic areas. However, despite consistent evidence showing major impairment in AT metabolism, as far as we know, no studies have addressed the possible relationship between metabolic and inflammatory AT modulation in progressive cachexia—in particular, in samples from the mesenteric depot—in that subcutaneous and omental depot have most often been used in studies on cachexia and AT remodeling.

To obtain greater insight into AT remodeling during the development of cancer-related cachexia and also into the possible association between Adl turnover and inflammatory profile, we have analyzed the mesenteric AT (MeAT) depot in tumor-bearing (TB) rats at early and cachetic stages and in patients with cancer, to allow for some translational data. As cachexia has been proposed to consist of 3 stages (21), efforts to detect the primary changes in the earlier cachexia stages may provide the basis for future intervention, hence preventing refractory disease.

We thus present results regarding the time course of Adl turnover and the pathways that may be involved in the progression of cachexia. Furthermore, we examined the presence of inflammatory cells during the development of cachexia and the association between infiltration and the alterations of the parameters of interest. Our findings indicated a discrete early impairment in the uptake and synthesis of fatty acids (FAs), followed by an increase in inflammatory cell infiltration and lipolysis, which become more evident in the cachexia stage. These results also suggest that the AT remodeling induced by CC consists of a non-resolving aseptic inflammation triggered by an impaired early Adl turnover, induced by CC.

MATERIAL AND METHODS

Animals

Male adult Wistar rats (200–280 g), obtained from the Central Animal House of the University of Mogi das Cruzes, were maintained in plastic cages, under controlled temperature conditions (22 ± 1°C), receiving water and food *ad libitum* (NuvilabCR1-Nuvital; Curitiba, Paraná, Brazil). The University of Mogi das Cruzes Ethics Committee for Animal Research approved all the adopted procedures. To induce CC, we injected Walker 256 tumor cells (2×10^7 cells) subcutaneously into the right flank of animals (5, 18). The animals were held in collective cages, containing 5 animals/cage. Body weight was assessed daily, and food intake on d 7 and 14 after injection, both always in the afternoon. To record the development of CC, experiments were performed in the time-course study when rats were killed by decapitation after 12 h of food withdrawal on d 0, 4, 7 (early stage) or 14 (cachexia stage) after injection (5–8 animals at each time point). Animals without tumor inoculation and with only vehicle solution were used as controls.

Blood samples and AT collection

After decapitation, trunk blood was collected into 15-ml conical-bottom Falcon tubes containing EDTA (1.8 mg/ml of blood) and centrifuged at 500 g for 10 min, and the plasma was separated and stored at −80°C. MeAT (after carefully dissecting of the adjacent lymph nodes) was removed, weighed, snap frozen in liquid nitrogen, and stored at −80°C.

Patients and sample collection

Patients were recruited between November 2008 and July 2010 at the University Hospital of the University of São Paulo (n = 12). The inclusion criteria were no prior cancer treatment and willingness to participate. The exclusion criteria were chemotherapy at the time of the study; continuous anti-inflammatory therapy; kidney or liver failure; and acquired immunodeficiency syndrome, inflammatory bowel disease, or chronic inflammatory processes not related with cachexia, including autoimmune disorders. The study was approved by the Human Ethics Committee of the University of São Paulo Hospital (CEP-ICB/USP 1117/13, CEP-HU/USP 752/07, and 1117/13, CAAE 0031.0.198.019-07). The patients were separated into 3 groups, based on diagnosis after surgery (22). They were subdivided into CC (n = 7), weight-stable cancer (WSC; n = 4) and (noncancer) control (n = 5) groups. The patients were considered cachectic based on criteria from the international consensus (20). Cachexia was defined as weight loss >5% during the past 6 mo or any degree of weight loss >2% the during the past 6 mo with body mass index (BMI) < 20 kg/m^2. The stable-weight groups were regarded as those with no important weight change during the past year and BMI < 25 kg/m^2. In the cancer groups (CC and WSC), the tumor primary location was the colon (n = 3), stomach (n = 2), and pancreas (n = 2). The control group included patients undergoing surgery for

incisional hernia ($n = 3$) and chronic cholecystitis ($n = 2$). The study was designed as intention to compare; therefore, all subjects were kept in the analyses, despite a few missing measurements.

Mesenteric white AT (~1 g, by approximate anatomic site), was collected within a 5-min interval, by a process similar to that described elsewhere (12). This procedure presents a minimal degree of risk and does not interfere with the standard surgery procedure. Clinical parameters of the patients were also collected as described previously (12). Tumor staging was determined after surgery according to the guidelines of the Union for International Cancer Control (UICC) TNM (tumor site, lymph node involvement, and metastatic spread) classification system (23).

General biochemical parameters in rats

The concentration of TG, glucose, and total protein were measured with commercial kits (Labtest, Lagoa Santa, Brazil).

Stromal vascular fraction isolation

Fragments of AT samples were placed in digestion buffer [DMEM; Sigma-D5671, 5% bovine serum albumin (BSA), 2 mg/ml collagenase type II (Thermo Fisher Scientific, Waltham, MA, USA)] and digested for 30 min at 37°C. After that, samples were centrifuged at 200 rpm for 30 s at room temperature. The pellet [stromal vascular fraction (SVF)] was snap frozen in liquid nitrogen and stored at −80°C.

Immunohistochemistry

MeAT samples were fixed in HistoChoice MB (Amresco, Solon, OH, USA) for 3 h at room temperature. Deparaffinized sections (5 μm) were incubated with 0.3% H_2O_2 in methanol for 5 min (until quenching of endogenous peroxidase activity and blocking of free protein-binding sites with 5% normal goat serum). Sections were immunostained for immune cells, with the following primary antibodies: anti-CD11b (ab75476); anti-CD68 (KP1; ab955); anti-TNFα (ab6671); anti-HSL (ab45422); anti-FASN (3180); and anti-iNOS2 (ab3523) (all from Cell Signaling Technology, Danvers, MA, USA). Specific secondary antibodies were polymer peroxidase, using Histofine Simple Stain Max-PO (Nichirei Biosciences, Tokyo, Japan). Histochemical reactions were performed with Sigma Fast 3,3-diaminobenzidine as the substrate (Sigma-Aldrich, St. Louis, MO, USA). Sections were counterstained with hematoxylin.

Real-time quantitative PCR

Total RNA was isolated from MeAT samples by using the RNeasy Lipid Tissue Mini Kit (Qiagen, Hilden, Germany), according to the manufacturer's recommendations. Complementary DNA synthesis was performed with 10 μl assay mix containing 2 μg total RNA. The reaction mixture was stored at −80°C until the PCR step. The following primers were used: C-X-C motif chemokine ligand (CXCL)2 (forward, 5′-AATGCCTGACGATACC-3′ and reverse, 5′-GAGTGGCTATGACTTCTGTCTGG-3′); C-C motif chemokine ligand (CCL)-5 (forward, 5′-ATATGGCTCGCACACCACTC-3′ and reverse, 5′-TGACAAAGACGACTGCAAGG-3′); CCL3 (forward, 5′-CGGTTTCTCTTGGTCAGGAA-3′ and reverse, 5′-CTTCTCCTATGGACGGCAAA-3′); CCL2 (forward, 5′-AATGAGTCGGCTGGAGAACTAC-3′ and reverse, 5′-CTCACTTGGTTCTGGTCCAGTT-3′); CD11C (forward, 5′-AGGTGTTGCTCCTGAGTGAG-3′ and reverse, 5′-TGCCTGGGCTCTCAGAAATG-3′); IL10 (forward, 5′-ACGCTGTCATCGATTTCTCC-3′ and reverse, 5′-TGGCCTTGTAGACACCTTTG-3′); TNFα (forward, GCTCCCTCTCATCAGTTCCA-3′ and reverse, 5′-GCTTGGTGGTTTGCTACGAC-3′); and arginase (forward, 5′-GGAAGAAAAGGCCCATTCAC-3′ and reverse, 5′-CTGTAAGGTAGGCCTCCCACA-3′). The results for mRNA concentrations were expressed as a ratio over RPL-19, which was amplified as a housekeeping gene, adopting the following primers: RPL-19 (forward, 5′-GGGAAGAGGAAGGGTACTGC-3′ and reverse, 5′-GACGGTCAATCTTCTTAGATTCC-3′). Analyses of real-time RT-PCR products were performed with the Prism 7500 SDS software (Thermo Fisher Scientific). Relative quantification of mRNA amount was obtained by the $2^{-\Delta\Delta Ct}$ method (24).

Western blot analysis

Frozen tissue was homogenized in RIPA buffer. Homogenates were centrifuged at 13,500 *g* for 20 min at 4°C, the supernatants (fatty layers) were discarded, and the infranatant was saved. Samples containing 50 μg protein were separated by electrophoresis on a 10% SDS-polyacrylamide gel. Proteins were then transferred to PVDF membranes at 100 V for 1 h. PVDF membranes were then blocked in Tris-buffered saline (TBS) containing 0.1% Tween 20 and 5% milk for 70 min. The PVDF membranes were incubated with primary antibodies (all from Cell Signaling Technology) against acetyl-CoA carboxylase (ACC; 3662; 1:2000); p-ACC (Ser79; 3661; 1:1000); HSL LIPE (ab45422; 1:4000); p-HSL Ser565 (4137; 1:2000); p-HSL Ser660 (4126; 1:4000); FASN (3180; 1:1000), ATGL (2138; 1:2000); AMPK (25322; 1:2000); and p-AMPK (Thr172; 2531; 1:2000), all overnight. The membranes were incubated with the secondary antibodies goat anti-rabbit IgG conjugated to horseradish peroxidase (HRP; 7074; 1:3000; Cell Signaling Technology) for 1 h at room temperature and were detected by ECL Prime (Amersham, Little Chalfont, United Kingdom). For the control of protein loading and transfer, we used Ponceau staining of the membranes. Quantification of the antigen–antibody complex was performed by the ImageJ Analysis Software (National Institutes of Health, Bethesda, MD, USA).

ELISA

The level of TNFα in serum was quantitated by ELISA (DuoSet ELISA; R&D Systems, Minneapolis, MN, USA), according to manufacturer's instructions. The optical density was measured at OD 450 nm (Synergy H1 Hybrid Reader; Biotek, Winooski, VT, USA).

Insulin tolerance test

The tests were performed at 8:00 AM after food had been withheld for 12 h. In 11-wk-old animals under light anesthesia (sodium thiopental; 2 mg/100 g of body weight), insulin was loaded (75 mU/100 g) and injected as a bolus, and blood glucose levels were determined at 0, 5, 10, 15, 30, 45, 60, and 90 min after injection.

Lipolysis assay

Isolated adipocytes were suspended in 40 μl of Kreb's/Ringer/phosphate buffer (pH 7.4, with 1% BSA) in 0.6 ml microtubes with 20 μl of adenosine deaminase (0.2 U/ml) and were incubated at 37°C for 5 min (as to degrade endogenously released adenosine). For additional analyses of the effect of TNFα on lipolysis, the same cells were stimulated

with 100 ng/ml TNFα for 12 h. Afterward, the cells were incubated for 1 h at 37°C either in presence of isoproterenol (β-adrenergic agonist) for determination of glycerol concentration (25). The concentration in the medium of released glycerol was quantified with a commercially available reagent (Sigma-Aldrich), measured according to the manufacturer's instructions.

Lipogenesis assay

Isolated adipocytes were suspended at 1:5 volume in Krebs/Ringer/phosphate buffer pH (pH 7.4, with 1% BSA with 2 mM glucose) at 37°C and saturated with a gas mixture of CO_2 (5%)/O_2 (95%). Aliquots (450 μl) were transferred to polypropylene test tubes (17 × 100 mm) containing 5 μl (0.05 μCi/tube) of D-[U-^{14}C]-glucose, in the presence or absence of insulin (10 nM). The analyses were performed with minor modifications to a published procedure in Borges-Silva *et al.* (25).

Statistical analysis

Data were analyzed, according to specific measurement, by Student's *t* test, 1- and 2-way ANOVA, followed by Tukey's *post hoc* comparison tests, with Prism software 6.0 (GraphPad, La Jolla, CA, USA). A value of $P < 0.05$ was considered significant for all statistical tests. Data are expressed as means ± SEM.

RESULTS

Characterization of cachexia syndrome

To investigate the effects of CC on Adl turnover, Walker 256 tumor cells (2×10^7 cells) were injected subcutaneously into the right flank of the rats, and the progression of CC was assessed on d 4, 7 (early stage), and 14 (cachexia stage). It is important to emphasize that the controls were of the same age and were euthanized on the same days, to allow for the assessment of growth pattern and any other potential age-related changes. The effects noted when cachexia was established (d 14) consisted of body weight loss (10.3%; $P < 0.01$), accompanied by dyslipidemia, evidenced by increased plasma levels of triglycerides (34.3%; $P < 0.01$). Hypoglycemia, another of the described features of the syndrome was also observed [decrease in 17.6% in glycemic level ($P < 0.01$) in TB d 14 (TB14) rats in relation to controls (age-matched non-TB rats)], as shown in **Table 1**. After a very discrete effect of early cachexia detected in the insulin tolerance test on d 4, an established CC stage (d 14) showed accentuated insulin resistance, with no response to insulin stimulation over 90 min (Supplemental Fig. S1). Food intake for the groups over the 14 d of treatment was similar (data not shown).

De novo lipogenesis is reduced early in CC

In an attempt to evaluate the main metabolic alterations during the development of the syndrome, we analyzed the lipogenesis (on d 4 and 14) in isolated cells in response to insulin stimulation (**Fig. 1**). Isolated adipose cells from the MeAT depot were assessed for their ability to incorporate D-[U-^{14}C]-glucose into TG, having shown no changes in cachectic animals in either of the two experimental periods, compared with their respective controls (Supplemental Fig. S2). To obtain more information regarding Adl turnover, we also evaluated the incorporation of glucose into lipid and glycerol TG moieties. *De novo* lipogenesis was assessed by addressing the difference between insulin-stimulated and basal conditions. Cachectic rats (TB14), demonstrated a reduction of 73.5% ($P < 0.05$) in the incorporation of glucose into FAs, when compared with the control. Also, when comparing the TB and control groups at different experimental time points (d 4 and 14), the cells from the TB group lost their ability to respond to insulin stimulation because of cachexia. In the unstimulated (basal) condition, glycerol incorporation tended to be lower in TB rats than in controls ($P = 0.056$) on d 4 (Fig. 1*A*). Glucose in response to glycerol incorporation (glycerol synthesis from glucose) showed an increase on d 14 *vs.* 4 ($P < 0.005$) in both groups, indicating that this parameter was not modulated by cachexia (Fig. 1*B*). To deepen the lipogenic pathway analysis, we also assessed FASN, p-ACC (Ser79 to total), and p-AMPK (Thr172 to total) protein expression. AMPK phosphorylation was increased in TB14 rats ($P = 0.0056$) when compared with controls. FASN and p-ACC (Ser79) did not change at any time point analyzed (Fig. 1*C*).

TABLE 1. *General characteristics of animal groups during the development of CC*

Parameter	Tumor cell inoculation group			
	Control (d 4)	TB4	Control (d 14)	TB14
n	6	7	5	8
BW (g)	248.9 ± 11.2	234.4 ± 28.8	327.2 ± 21.7	293.5 ± 13.9*
Tumor weight (g)	–	2.4 ± 0.8	–	25.8 ± 2.7
BW increase (%)	–	–	31.5 ± 3.2	17.7 ± 1.9*
Glucose (mg/dl)	121.0 ± 12.2	121.3 ± 9.4	108.5 ± 12.7	102.9 ± 6.7†
TG (mg/dl)	84.22 ± 2.7	98.74 ± 6.6	91.81 ± 7.1	139.8 ± 23.6*
Total protein (g/dl)	4.48 ± 0.1	4.59 ± 0.2	4.44 ± 0.2	4.32 ± 0.1

*$P < 0.05$ *vs.* control (d 14); †$P < 0.05$ *vs.* control (d 4).

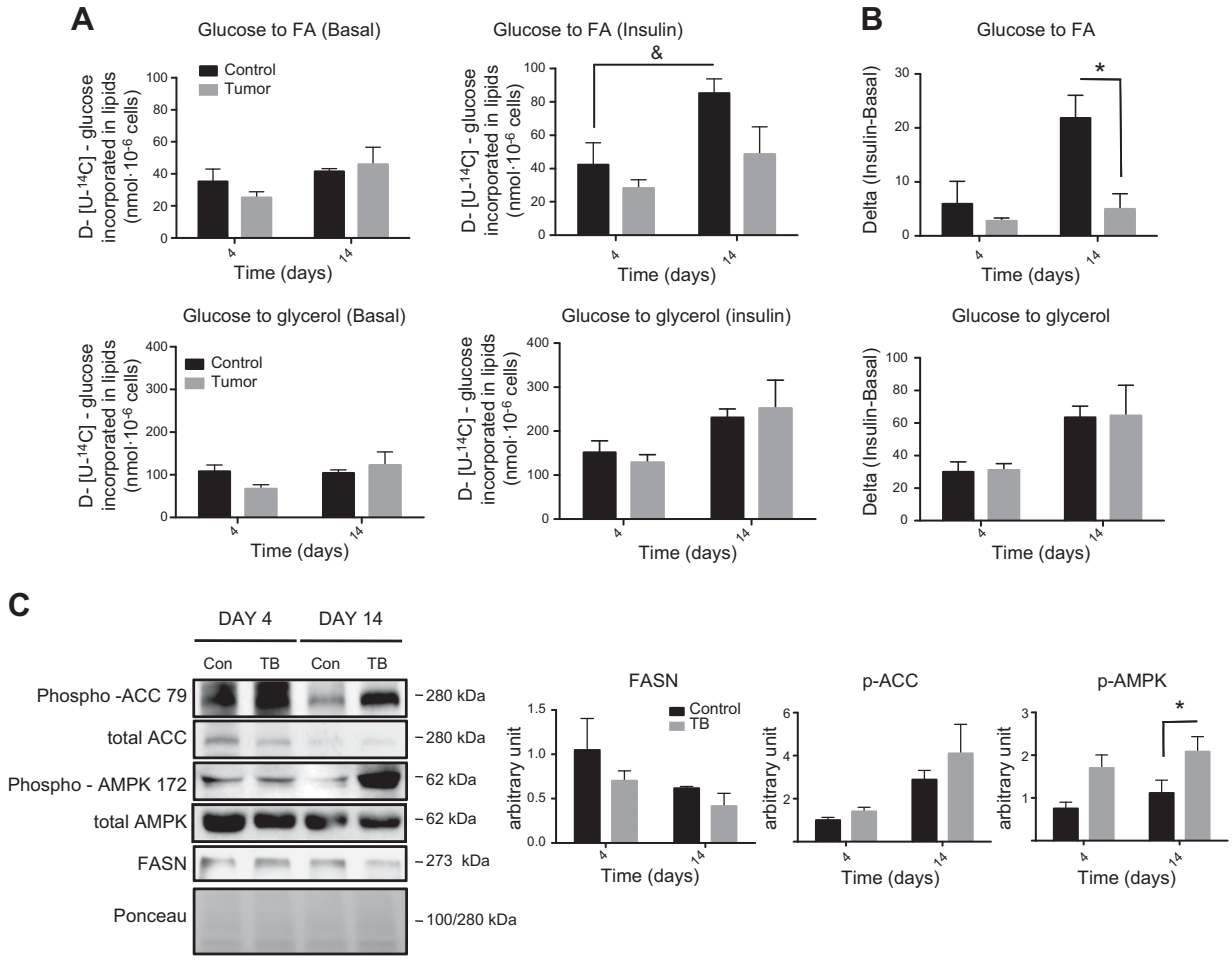

Figure 1. Lipogenesis modulation during CC. *A*) Basal and insulin-stimulated lipogenesis. *B*) Variation (Δ) of basal and insulin-stimulated conditions. *C*) Immunoblot analysis for components of lipogenesis pathway from MeAT on d 4 and 14 after tumor cell inoculation. Blots were rearranged, and representative images were selected for p-ACC (Ser79), ACC, p-AMPK (Thr172), AMPK, and FASN and Ponceau Red staining (normalized protein). Values are means ± SEM (5–8 animals at each time point). $^{\&}P < 0.05$, time effect (d 4 *vs.* 14); $^{*}P < 0.05$, tumor effect (TB *vs.* control).

To evaluate parameters related to the uptake of FAs and structural proteins of the lipid droplets, we also analyzed the gene expression of LPL, cell death-inducing DFFA-like effector (CIDE)-A, and CIDEC (Supplemental Fig. S3). Decreases of 44% ($P < 0.05$) on d 4, and of 56% ($P < 0.05$) on d 14 were observed in LPL gene expression from MeAT from TB rats. Furthermore, the structural protein markers of lipid droplets behaved similarly: CIDEA showed a 35% reduction ($P < 0.05$) on d 4 and a 69% reduction ($P < 0.05$) on d 14, whereas CIDEC was reduced by 53% only on d 4 ($P < 0.05$).

Lipolysis is related to increased levels of p-HSL Ser660

Lipolysis is the catabolic branch of the FA cycle that provides FAs in times of metabolic need. Lipogenesis is the anabolic branch that removes FAs when they are present in excess. In the cachexia stage, lipolysis is the most well-described event, responsible for disruption in Adl turnover. In relation to the adipocyte basal rates of lipolysis (unstimulated), we observed an unexpected decrease in glycerol release in TB4 rats in relation to the control group on d 4 (63.9%; $P < 0.001$), followed by an increase in p-HSL (Ser565) expression (78.1%; $P < 0.05$), which inhibits HSL activity. During cachexia development, an increase on d 14 in the TB group was demonstrated in relation to the control group (46.8%; $P < 0.05$) (**Fig. 2*A***). Isoproterenol stimulation in isolated adipocytes induced an increase of 62.1% ($P < 0.01$) that was observed, only in TB animals (d 4 × 14). In the cachexia stage, increased lipolysis was paralleled by increased levels of both p-HSL (Ser660) protein expression, in the MeAT samples, and nonesterified FAs, in the plasma from cachectic TB14 rats. No changes were detected in p-HSL (Ser565) and ATGL protein expression (Fig. 2*B*) in the cachexia stage.

Cachexia induces a temporal increase in immune cell infiltration

AT inflammation is another feature recently demonstrated in the AT remodeling process induced by CC (10, 19). However, there is no information regarding

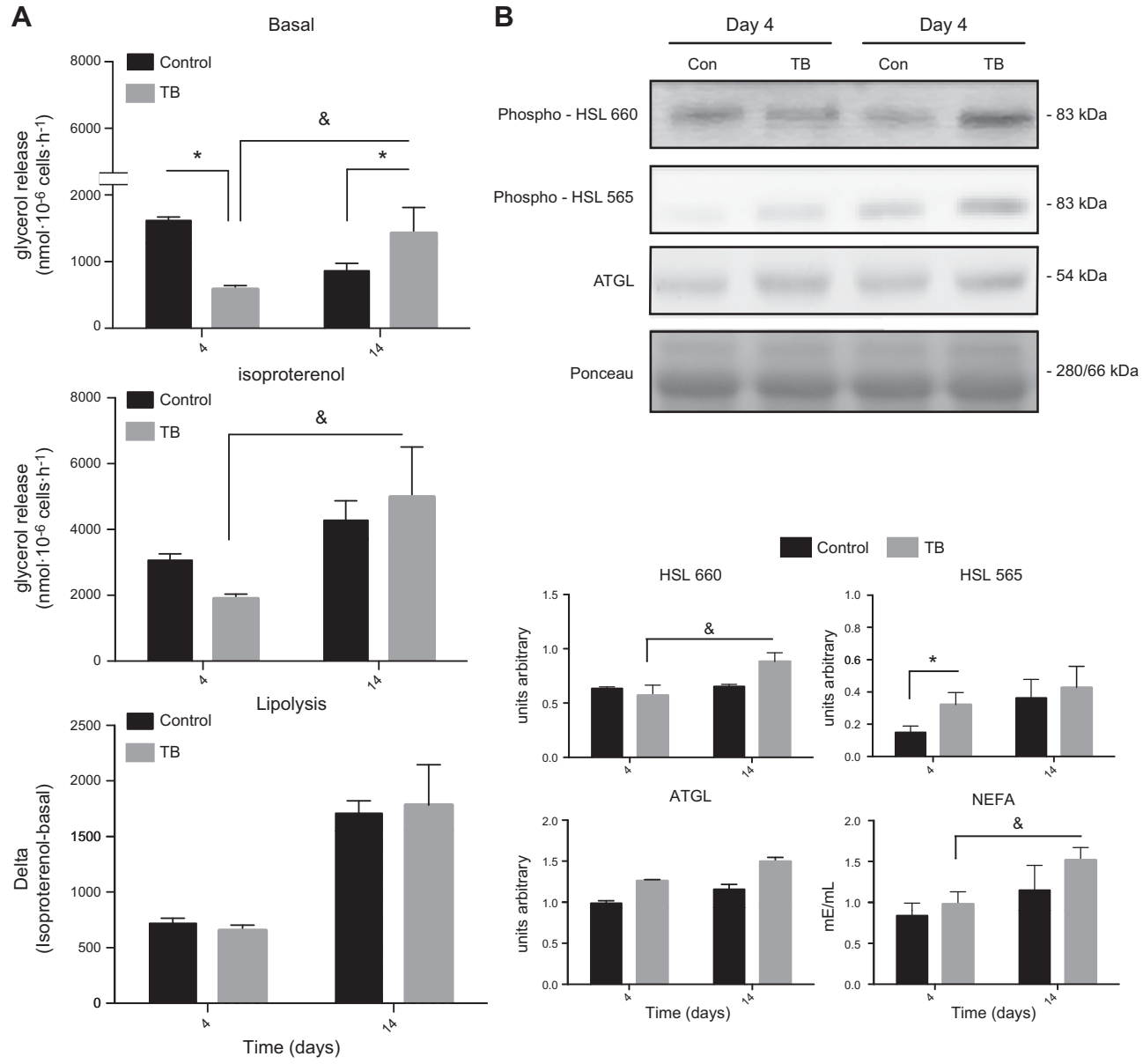

Figure 2. Lipolysis modulation during CC. *A*) Basal and isoproterenol-stimulated lipolysis and variation of stimulated and basal conditions (Δ). *B*) Immunoblot analysis for components of lipolysis from MeAT on d 4 and 14 after tumor cell inoculation. Blots were rearranged, and representative images were selected for HSL, p-HSL (Ser660), p-HSL (Ser565, and ATGL and Ponceau Red staining (normalized protein). Values are means ± SEM (5–8 animals at each time point). $^{\&}P < 0.05$, time effect (d 4 *vs.* 14); $^{*}P < 0.05$, tumor effect (TB *vs.* control).

acute and chronic inflammatory events in this scenario, nor any yet described connection with impairment of metabolic parameters and inflammation. Thus, we evaluated the presence of $CD11b^+$ cells (neutrophil marker), as well as the presence of $CD68^+$ cells (macrophages) during CC (**Fig. 3*A***). Immunostaining for CD11b was detected only in TB7 rats, with no detection in TB14 rats. CD68-positive cells were detected only on d 14. Considering the profile of the appearance of inflammatory cell infiltrate associated with cachexia observed in this study, we also aimed to verify specific chemoattractants for polymorphonuclear cells: CCL3 and CXCL2, as well as CCL2, for macrophages. CCL3 and CXCL2 expression was increased ~7.2 and 9.7-fold, respectively ($P < 0.01$), only in TB7 rats after inoculation of tumor cells, in the SVF from MeAT, when compared with controls, and no changes were detected in TB14 rats. CCL2 showed increased (10.1-fold; $P < 0.01$) gene expression only in the MeAT from TB14 rats (Fig. 3*B*). Furthermore, in cachectic TB14 rats, we found that these macrophages underwent polarization to the M1 phenotype, in view of the high expression of CD11c and arginase found in TB14 rats (10.8- and 3.1-fold, respectively; $P < 0.01$; Fig. 3*C*).

TNFα is related to increased lipolysis in CC

Plasma levels of TNFα in TB14 rats showed a 2.0-fold increase compared with the controls. Having detected an

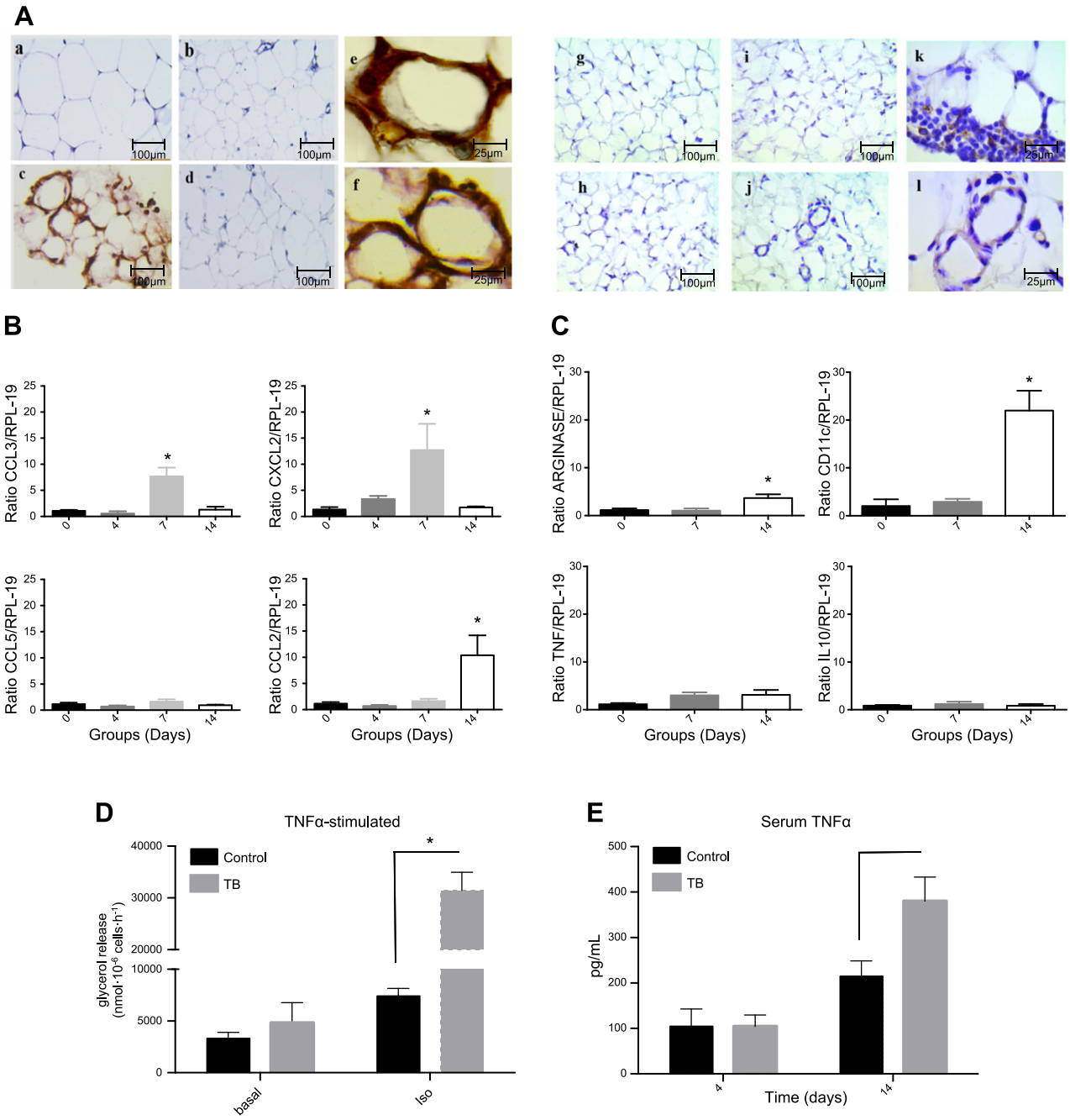

Figure 3. AT inflammatory profile during CC. *A*) Immunohistochemistry (IHC) of MeAT sections stained with CD11b [left panels: *a*) d 0 (control); *b*) d 4; *c*) d 7; *d*) d 14; *e*, *f*) d 7] and CD68 [right panels: *g*) d 0 (control); *h*) d 7; *i*) d 4; *j*–*l*) d 14]. *B*) Quantitative PCR of mRNA gene expression of cell infiltration markers (CCL2, CCL3, CCL5, and CXCL2) from SFV of MeAT. *C*) Quantitative PCR of mRNA gene expression of a macrophage polarization (arginase, TNFα, CD11c, and IL10) from SFV of MeAT. *D*) Isolated adipocytes stimulated with 100 ng/ml TNF-α for 12 h. After that period, lipolysis was induced and determined by glycerol release by isolated adipocytes from cachectic rats (d 14). *E*) Change in level of TNFα in serum on d 4 and 14 after tumor cell inoculation. TNFα levels in serum were measured by ELISA. Values are means ± SEM (5–8 animals at each time point). Iso, isoproterenol. $^*P < 0.05$ *vs.* control.

immunometabolic disruption in TB14 rats, characterized by an increased presence of inflammatory cells, macrophages in particular, which was concomitant to increased lipolysis, we performed an experiment to determine whether TNFα actually contributes to the lipolytic effect observed in cachexia (Fig. 3*D*, *E*). We measured glycerol released (basal and Isoproterenol-stimulated) in isolated adipocytes cultured over 12 h with TNFα (100 ng/ml) in both groups (control and TB). A comparison of the values found in the response (to TNFα stimulus) with those of the basal condition showed a high increase (6.5-fold) in glycerol release in TB14 rats, as compared to the matching control group (d 14).

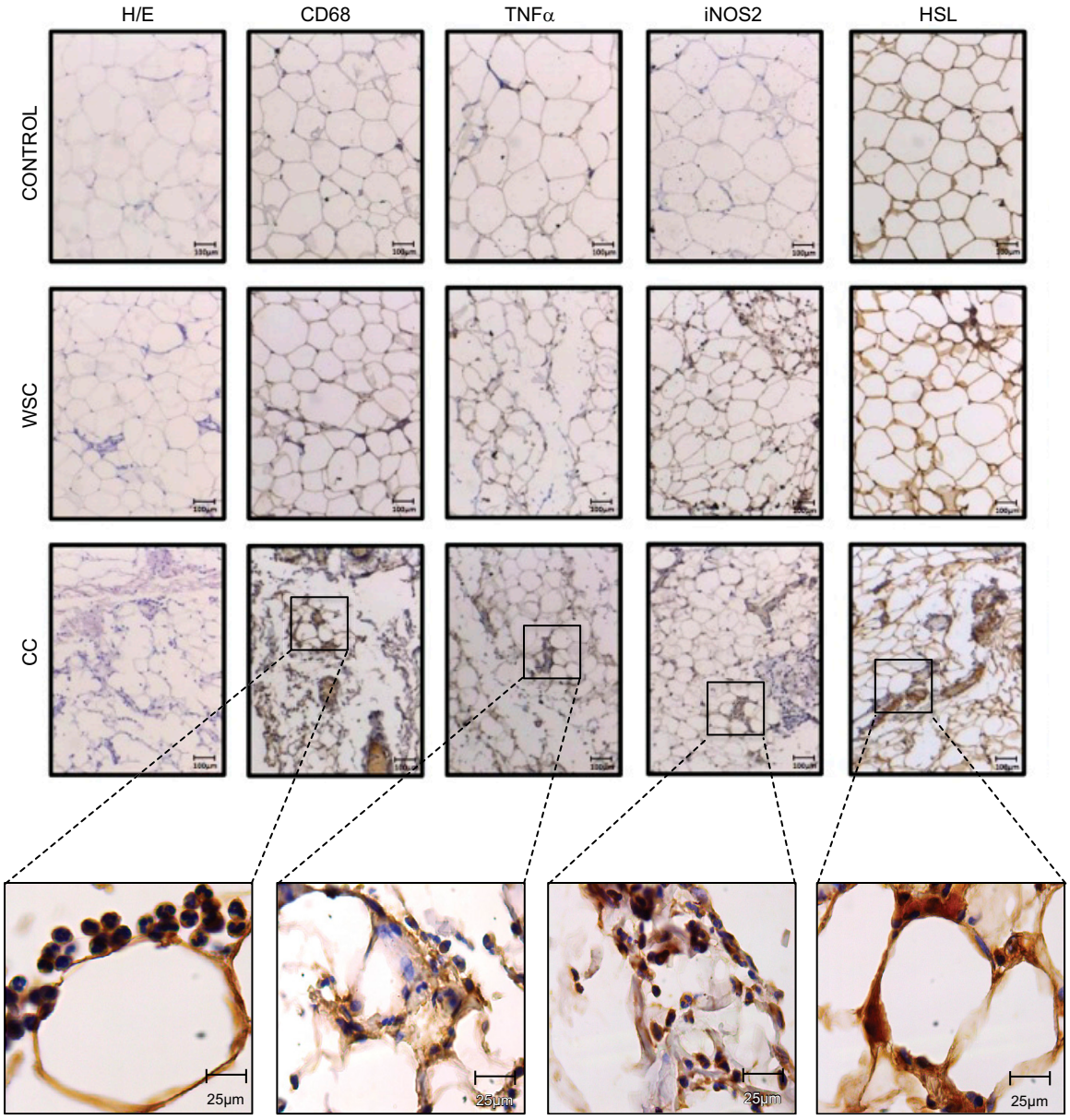

Figure 4. Histologic analysis and immunohistochemistry (IHC) of MeAT from patients with CC. Tissue sections were stained with H&E; representative IHC sections were stained with CD68 and iNOS2 (infiltrated cells), TNFα (inflammation), and HSL (lipolytic markers). Tissue sections were counterstained with hematoxylin. The brown staining represents the indicated antigen, and blue is the nuclear counterstain.

Patients with CC show immunometabolic disarrangement in MeAT

To investigate whether similar findings would be found in patients, the presence of infiltrated cells (CD68 and iNOS2), inflammation (TNFα), and lipolytic markers (HSL) in the MeAT obtained from patients with CC (**Fig. 4**) was studied. An increased density of $CD68^+$ cells was observed in the CC group. We also found increased $iNOS2^+$ cells, suggesting that these macrophages were polarized to M1. An increased number of $TNF\alpha^+$ cells in the CC were also detected, as well as an increase in the presence of HLS^+ cells. HSL staining was detected in the area with the higher presence of infiltrated cells in the CC group, suggesting possible immunometabolic modulation during human cachexia. The subjects in the 3 groups were of similar age and BMI (data not shown). The CC group showed values ranging from 6 to 23% of body weight loss in the previous 6 mo and C-reactive protein ranging from 4.6 to 11.9 μg/ml, indicating that we studied cachexia staging in patients. Regarding the patients with WSC, there was no significant body weight change in the previous 6 mo, and C-reactive protein values ranged from 1.4 to 5.8 μg/ml.

DISCUSSION

Cachexia induces profound immunometabolic changes that result in an impairment of AT function in CC, a process characterized by AT remodeling (10, 14, 20). We

investigated the role of Adl turnover and inflammation of MeAT, and we demonstrated early metabolic changes, especially those related to *de novo* lipogenesis, indicating a discrete and silent disruption in Adl turnover. At the cachexia stage (d 14), disruption in Adl turnover was accentuated, as shown by the impaired ability to synthesize lipids from glucose (*de novo* lipogenesis), as well as by the increased lipolysis. Another interesting aspect was the inflammatory profile of MeAT, with increased neutrophil leukocyte infiltration (acute inflammatory signals), followed by macrophage infiltration in fully established cachexia. The translational approach adopted herein enabled the finding that the immunometabolic profile observed in the animal model was also present in MeAT obtained from patients with CC. Finally, lipolysis was progressively enhanced during the development of cachexia, and TNFα seemed to play a relevant role as a modulator of this pathway, notably during the more advanced stage of the disease.

Adl turnover has been characterized in human obesity, by a consistent predominance of lipogenesis over lipolysis (26). In CC, few studies have addressed this question, and most of them have evaluated the mechanisms behind the typically increased lipolysis. However, recently, an early down-regulation of lipogenic genes was shown in an animal model of cachexia (Walker 256) (5). In addition, in the cachexia stage, accentuated reduction in *de novo* lipogenesis from adipocytes was the most prevalent finding. Those changes were followed by the down-regulation of LPL gene expression, already evident from the early cachexia stage (d 4), in addition to AMPK activation. In particular, this effect was shown to be consistently present in CC, indicating that modulation of Adl turnover during early stages of the syndrome may be associated with activation of AMPK in Walker 256 TB rats. In this respect, a recent study demonstrated activation of AMPK during cachexia in C-26 TB rats (27). Such activation is related to reduced transcript levels of LPL, Ap2, and CD36 in cachectic rats, suggesting some degree of repression in the uptake or intracellular handling of FAs—hence, demonstrating impairment of *de novo* lipogenesis.

Taking into account that the deregulation of Adl turnover is the basis for the development of the cachectic condition, we also assessed several steps in the lipolytic pathway in AT. In TB rats, the deregulation of lipolysis (*in vitro*) revealed a distinct profile, depending on the degree of disease progression—that is, in an early stage (d 4) or in a more advanced stage of cachexia (d 14). In the first, the basal rate of lipolysis was reduced and was accompanied by increased p-HSL (Ser565) expression, which is regulated by AMPK activation and consequently, inhibits HSL activity (28). Patients with CC show reduced spontaneous basal lipolysis with elevated *ex vivo* responses to catecholamines and natriuretic peptides (14). On the other hand, there is no information regarding the stage of cachexia in such patients, and possible translational correlation is limited.

During the cachexia stage (d 14), adipocytes from TB rats exhibited increased rates of lipolysis under both basal and stimulated situations. Of note, modulation of key regulators of the lipolytic pathway in cachexia correlate with several studies in humans and other animal models (5, 15, 27, 29). In particular, increased lipolysis in the advanced cachexia stage is a change described to be the most directly related to the central metabolic dysfunction of AT. We have been able to add further information concerning the modulation in adipose Adl turnover in TB animals during a period when cachexia was not as evident (d 4). However, further studies are needed to determine the role of early impairment on lipid turnover at different stages of cachexia.

AT has been implicated in chronic systemic inflammation that occurs during CC development, which has been proposed to present a relevant contribution from the AT, as we and others have already shown (10, 12, 18, 19). In this study, we described the presence of inflammatory cells in MeAT during different stages of CC. On d 7, a period when the classic signs of cachexia are not easily detected or diagnosed, there was an increase in the presence of neutrophils. Such an acute inflammatory event, involving a plethora of cachexia signals, suggests the existence of a precocious acute inflammatory signal in MeAT. In patients with cancer, increased expression of neutrophil-derived proteases from blood samples was recently demonstrated, both before and during cachexia, suggesting that these biomarkers contribute to the early diagnosis and prevention of cachexia (30). In addition, the presence of $CD68^+$ cells in MeAT seems to be followed by the polarization of macrophages developing into an activated M1 proinflammatory state, observed only in the advanced cachexia stage. However, additional studies are needed to confirm these observations.

In patients with cancer, modifications of macrophage infiltration and subphenotype profiles of AT were recently demonstrated (18). However, this characterization was undertaken in the subcutaneous depot with no information related to visceral depots—in particular in the mesenteric depot. In fact, in AT, during atrophy induced by cachexia, M1 macrophages infiltrate the tissue and may secrete proinflammatory molecules, such as TNFα, Il-1β, and IL-6, which, in turn, may modulate Adl turnover. In this respect, TB animals showed, simultaneous with body weight loss, dyslipidemia and AT inflammation and increased levels of serum TNFα in the advanced cachexia stage. Moreover, adipocytes from TB animals were more sensitive to the magnitude of isoproterenol stimuli and demonstrated higher lipolytic response when cultured with TNFα.

In general, one feature of AT inflammation is enhanced local release of TNFα, which originates from fat cells and nonfat cells within AT (18). Although other cytokines/chemokines are also released within AT, only TNFα has a pronounced lipolytic effect in human adipocytes (31). To the best of our knowledge, we have shown, for the first time, that an increase in tissue and systemic TNFα levels may be an important factor for modulating lipolysis in CC, at least in Walker 256 TB animals. However, not only increased production and secretion of TNFα, but also alterations in its signal transduction pathways activated by the cytokine may be essential for the increased lipolysis observed in development of cachexia (14, 32).

To add translational data to this study, we analyzed, in MeAT, inflammatory and metabolic (immunometabolic) parameters from patients with CC. Such a modification was followed by the presence of CD68-labeled AT macrophages localized to crowns surrounding adipocytes, similar to what we had previously reported for subcutaneous AT samples (10). As far as we know, although this structure has already been described in subcutaneous AT samples, this is the first time that it has been described in such visceral AT samples. Also, with regard to the metabolic parameters, an increased HSL-labeled cell presence in the AT from patients with CC appears to be accentuated in areas with the higher accumulation of infiltrating inflammatory cells. In patients with cancer, elevated HSL mRNA and protein levels from subcutaneous AT have been shown to contribute to increased lipolysis (29). However, further studies are needed to determine the possible lipid turnover disruption in AT from different groups of patients with cancer at different stages during the development of the disease.

The limitations of the study should be acknowledged. We performed a descriptive analysis of the time course of cachexia development in the Walker 256 tumor experimental model of induced cachexia. The same immunometabolic modification observed in the AT, evident in both animals and patients with cancer, should be extended into different experimental models of cachexia. Regarding patients with cancer, we performed qualitative analyses in a limited number of patients with CC. We have not attempted to adopt this staging system to classify cachexia, because of the relatively small sample.

In summary, translational analysis of MeAT from patients and an animal model of CC enabled us to identify the very early changes in Adl turnover and the subsequent inflammatory response profile associated with AT remodeling induced by cachexia. Our results shed new light on the putative mechanisms behind the early and discrete impairment of AT lipid metabolism during the development of AT atrophy and the cachexia process, suggesting that aseptic inflammation may be triggered by an impaired Adl turnover in this setting. Such disruption is already evident, even before any detection of classic markers of inflammatory response, characterized by an increase in M1 phenotype macrophages in the advanced cachectic stage. Thus, together with our novel findings, the ability of TNFα to potentiate the effect of isoproterenol inducing lipolysis during advanced cachexia may be useful in elucidating the mechanisms underlying AT dysfunction in this syndrome, as well as in providing insight to the development of new strategies intended to prevent or mitigate this condition. FJ

ACKNOWLEDGMENTS

This work was sponsored by São Paulo Research Foundation (FAPESP) Grants: 2010/51078-1 (to M.L.B.), 2012/500790-0 (to M.S.), and 2015/19259-0 (to M.L.B.) and CNPq 311966/2015-2 (to M.L.B.). The authors thank Dr. José Pinhata Otoch and Dr. Paulo S. M. de Alcântara and team for their excellent support and assistance in clinical data management and acquisition. The contents of this article are solely the responsibility of the authors and do not necessarily represent the official views of FAPESP. The authors declare no conflicts of interest.

AUTHOR CONTRIBUTIONS

M. L. Batista, Jr., M. Seelaender, and F. B. Lima designed the research; F. S. Henriques, R. A. L. Sertié, F. O. Franco, R. X. Neves, S. Andreotti, and P. Knobl performed the research; M. Seelaender, F. B. Lima, and A. Guilherme contributed new reagents or analytic tools; A. Guilherme, F. S. Henriques, and F. O. Franco analyzed the data; and M. L. Batista, Jr., M. Seelaender, and F. S. Henriques wrote the paper.

REFERENCES

1. Tsoli, M., Swarbrick, M. M., and Robertson, G. R. (2016) Lipolytic and thermogenic depletion of adipose tissue in cancer cachexia. *Semin. Cell Dev. Biol.* **54**, 68–81
2. Arner, P. (2011) Medicine: lipases in cachexia. *Science* **333**, 163–164
3. Gullett, N. P., Mazurak, V. C., Hebbar, G., and Ziegler, T. R. (2011) Nutritional interventions for cancer-induced cachexia. *Curr. Probl. Cancer* **35**, 58–90
4. Argilés, J. M., Busquets, S., Stemmler, B., and López-Soriano, F. J. (2014) Cancer cachexia: understanding the molecular basis. *Nat. Rev. Cancer* **14**, 754–762
5. Batista, M. L., Jr., Neves, R. X., Peres, S. B., Yamashita, A. S., Shida, C. S., Farmer, S. R., and Seelaender, M. (2012) Heterogeneous time-dependent response of adipose tissue during the development of cancer cachexia. *J. Endocrinol.* **215**, 363–373
6. Kliewer, K. L., Ke, J. Y., Tian, M., Cole, R. M., Andridge, R. R., and Belury, M. A. (2015) Adipose tissue lipolysis and energy metabolism in early cancer cachexia in mice. *Cancer Biol. Ther.* **16**, 886–897
7. Ebadi, M., and Mazurak, V. C. (2014) Evidence and mechanisms of fat depletion in cancer. *Nutrients* **6**, 5280–5297
8. Kir, S., White, J. P., Kleiner, S., Kazak, L., Cohen, P., Baracos, V. E., and Spiegelman, B. M. (2014) Tumour-derived PTH-related protein triggers adipose tissue browning and cancer cachexia. *Nature* **513**, 100–104
9. Petruzzelli, M., Schweiger, M., Schreiber, R., Campos-Olivas, R., Tsoli, M., Allen, J., Swarbrick, M., Rose-John, S., Rincon, M., Robertson, G., Zechner, R., and Wagner, E. F. (2014) A switch from white to brown fat increases energy expenditure in cancer-associated cachexia. *Cell Metab.* **20**, 433–447
10. Batista, M. L., Jr., Henriques, F. S., Neves, R. X., Olivan, M. R., Matos-Neto, E. M., Alcântara, P. S., Maximiano, L. F., Otoch, J. P., Alves, M. J., and Seelaender, M. (2016) Cachexia-associated adipose tissue morphological rearrangement in gastrointestinal cancer patients. *J. Cachexia Sarcopenia Muscle* **7**, 37–47
11. Franco, F. O., Lopes, M. A., Henriques, F. S., Neves, R. X., Bianchi Filho, C., and Batista, M. L., Jr. (2017) Cancer cachexia differentially regulates visceral adipose tissue turnover. [E-pub ahead of print] *J. Endocrinol.* doi: 10.1530/JOE-16-0305
12. Batista, M. L., Jr., Olivan, M., Alcantara, P. S., Sandoval, R., Peres, S. B., Neves, R. X., Silverio, R., Maximiano, L. F., Otoch, J. P., and Seelaender, M. (2013) Adipose tissue-derived factors as potential biomarkers in cachectic cancer patients. *Cytokine* **61**, 532–539
13. Seelaender, M., Laviano, A., Busquets, S., Püschel, G. P., Margaria, T., and Batista, M. L., Jr. (2015) Inflammation in cachexia. *Mediators Inflamm.* **2015**, 536954
14. Arner, P., and Langin, D. (2014) Lipolysis in lipid turnover, cancer cachexia, and obesity-induced insulin resistance. *Trends Endocrinol. Metab.* **25**, 255–262
15. Das, S. K., Eder, S., Schauer, S., Diwoky, C., Temmel, H., Guertl, B., Gorkiewicz, G., Tamilarasan, K. P., Kumari, P., Trauner, M., Zimmermann, R., Vesely, P., Haemmerle, G., Zechner, R., and Hoefler, G. (2011) Adipose triglyceride lipase contributes to cancer-associated cachexia. *Science* **333**, 233–238
16. Fouladiun, M., Körner, U., Bosaeus, I., Daneryd, P., Hyltander, A., and Lundholm, K. G. (2005) Body composition and time course changes in regional distribution of fat and lean tissue in unselected cancer patients on palliative care: correlations with food intake, metabolism, exercise capacity, and hormones. *Cancer* **103**, 2189–2198

17. Murphy, R. A., Wilke, M. S., Perrine, M., Pawlowicz, M., Mourtzakis, M., Lieffers, J. R., Maneshgar, M., Bruera, E., Clandinin, M. T., Baracos, V. E., and Mazurak, V. C. (2010) Loss of adipose tissue and plasma phospholipids: relationship to survival in advanced cancer patients. *Clin. Nutr.* **29**, 482–487
18. De Matos-Neto, E. M., Lima, J. D., de Pereira, W. O., Figuerêdo, R. G., Riccardi, D. M., Radloff, K., das Neves, R. X., Camargo, R. G., Maximiano, L. F., Tokeshi, F., Otoch, J. P., Goldszmid, R., Câmara, N. O., Trinchieri, G., de Alcântara, P. S., and Seelaender, M. (2015) Systemic inflammation in cachexia: is tumor cytokine expression profile the culprit? *Front. Immunol.* **6**, 629
19. Neves, R. X. Rosa-Neto, J. C., Yamashita, A. S., Matos-Neto, E. M., Riccardi, D. M. R., Lira, F. S., Batista, Jr., M. L., and Seelaender, M. (2015) White adipose tissue cells and the progression ofcachexia: inflammatory pathways. *J. Cachexia Sarcopenia Muscle* **7**, 193–203
20. Bing, C., Russell, S., Becket, E., Pope, M., Tisdale, M. J., Trayhurn, P., and Jenkins, J. R. (2006) Adipose atrophy in cancer cachexia: morphologic and molecular analysis of adipose tissue in tumour-bearing mice. *Br. J. Cancer* **95**, 1028–1037
21. Fearon, K., Strasser, F., Anker, S. D., Bosaeus, I., Bruera, E., Fainsinger, R. L., Jatoi, A., Loprinzi, C., MacDonald, N., Mantovani, G., Davis, M., Muscaritoli, M., Ottery, F., Radbruch, L., Ravasco, P., Walsh, D., Wilcock, A., Kaasa, S., and Baracos, V. E. (2011) Definition and classification of cancer cachexia: an international consensus. *Lancet Oncol.* **12**, 489–495
22. Evans, W. J., Morley, J. E., Argilés, J., Bales, C., Baracos, V., Guttridge, D., Jatoi, A., Kalantar-Zadeh, K., Lochs, H., Mantovani, G., Marks, D., Mitch, W. E., Muscaritoli, M., Najand, A., Ponikowski, P., Rossi Fanelli, F., Schambelan, M., Schols, A., Schuster, M., Thomas, D., Wolfe, R., and Anker, S. D. (2008) Cachexia: a new definition. *Clin. Nutr.* **27**, 793–799
23. Kwon, S. J. (2011) Evaluation of the 7th UICC TNM staging system of gastric cancer. *J. Gastric Cancer* **11**, 78–85
24. Wex, T., Lendeckel, U., Wex, H., Frank, K., and Ansorge, S. (1995) Quantification of aminopeptidase N mRNA in T cells by competitive PCR. *FEBS Lett.* **374**, 341–344
25. Borges-Silva, C. N., Fonseca-Alaniz, M. H., Alonso-Vale, M. I., Takada, J., Andreotti, S., Peres, S. B., Cipolla-Neto, J., Pithon-Curi, T. C., and Lima, F. B. (2005) Reduced lipolysis and increased lipogenesis in adipose tissue from pinealectomized rats adapted to training. *J. Pineal Res.* **39**, 178–184
26. Arner, P., Bernard, S., Salehpour, M., Possnert, G., Liebl, J., Steier, P., Buchholz, B. A., Eriksson, M., Arner, E., Hauner, H., Skurk, T., Rydén, M., Frayn, K. N., and Spalding, K. L. (2011) Dynamics of human adipose lipid turnover in health and metabolic disease. *Nature* **478**, 110–113
27. Tsoli, M., Schweiger, M., Vanniasinghe, A. S., Painter, A., Zechner, R., Clarke, S., and Robertson, G. (2014) Depletion of white adipose tissue in cancer cachexia syndrome is associated with inflammatory signaling and disrupted circadian regulation. *PLoS One* **9**, e92966
28. Greenberg, A. S., Shen, W. J., Muliro, K., Patel, S., Souza, S. C., Roth, R. A., and Kraemer, F. B. (2001) Stimulation of lipolysis and hormone-sensitive lipase via the extracellular signal-regulated kinase pathway. *J. Biol. Chem.* **276**, 45456–45461
29. Agustsson, T., Rydén, M., Hoffstedt, J., van Harmelen, V., Dicker, A., Laurencikiene, J., Isaksson, B., Permert, J., and Arner, P. (2007) Mechanism of increased lipolysis in cancer cachexia. *Cancer Res.* **67**, 5531–5537
30. Penafuerte, C. A., Gagnon, B., Sirois, J., Murphy, J., MacDonald, N., and Tremblay, M. L. (2016) Identification of neutrophil-derived proteases and angiotensin II as biomarkers of cancer cachexia. *Br. J. Cancer* **114**, 680–687
31. Langin, D., and Arner, P. (2006) Importance of TNFalpha and neutral lipases in human adipose tissue lipolysis. *Trends Endocrinol. Metab.* **17**, 314–320
32. Guilherme, A., Virbasius, J. V., Puri, V., and Czech, M. P. (2008) Adipocyte dysfunctions linking obesity to insulin resistance and type 2 diabetes. *Nat. Rev. Mol. Cell Biol.* **9**, 367–377

Received for publication October 21, 2016.
Accepted for publication January 9, 2017.